Temperature-dependent dielectric properties of Au/Si_3N_4/n-Si (metal–insulator–semiconductor) structures*

T. Ataseven and A. Tataroğlu†

Physics Department, Faculty of Sciences, Gazi University, Teknikokullar, Ankara 06500, *Turkey*

(Received 20 January 2013; revised manuscript received 7 May 2013)

The dielectric properties of Au/Si_3N_4/n-Si (MIS) structures are studied using the admittance measurements (C–V and G/ω–V) each as a function of temperature in a range from 80 K to 400 K for two frequencies (100 kHz and 1 MHz). Experimental results show that both the dielectric constant (ε') and the dielectric loss (ε'') increase with temperature increasing and decrease with frequency increasing. The measurements also show that the ac conductivity (σ_{ac}) increases with temperature and frequency increasing. The $\ln\sigma_{ac}$ versus $1000/T$ plot shows two linear regions with different slopes which correspond to low (120 K–240 K) and high (280 K–400 K) temperature ranges for the two frequencies. It is found that activation energy increases with frequency and temperature increasing.

Keywords: Au/Si_3N_4/n-Si (metal–insulator–semiconductor) structure, admittance measurements, dielectric properties, ac conductivity

PACS: 73.40.Qv, 84.37.+q, 77.22.Ch, 72.20.–i **DOI:** 10.1088/1674-1056/22/11/117310

1. Introduction

The metal–semiconductor (MS) structure has become an important and essential part of semiconductor devices, and studies of it are vital to the development of technology.[1–8] The existence of an interfacial insulator layer between the metal and semiconductor converts the MS structure into a metal–insulator–semiconductor (MIS) structure. As is well known, the interface traps at the semiconductor–insulator interface in the MIS structure play an important role in determining several characteristics of electronic devices utilizing this structure. The admittance (capacitance and conductance) measurements of MIS structures have been extensively studied to investigate the effects of the interfacial layer on the electrical and dielectric characteristics of the MIS structure.[7–13] Analyses of the electric and dielectric parameters of these devices only at room temperature have not provided detailed information about their conduction processes.

In recent years, silicon nitride (Si_3N_4) films have been examined as a potential material to replace silicon dioxide (SiO_2) in such structures.[13–18] Compared with silicon dioxide, silicon nitride was expected to be a more stable dielectric layer on silicon. Furthermore, silicon nitride has become a promising material for replacing SiO_2 in metal oxide-semiconductor transistors and storage capacitors to reduce the device scales of integrated circuits in microelectronic applications. Si_3N_4 films were also used as an essential part in MIS inversion layer solar cells, having applications as antireflection and passivation coatings as well as in the active layer, causing energy band bending.[19,20]

In our previous study,[12] we reported on the frequency dependences of electrical and dielectric properties of the Au/Si_3N_4/n-Si (MIS) structures. The capacitance–voltage (C–V) and conductance–voltage (G/ω–V) characteristics have been measured in a frequency range of 1 kHz–1 MHz at room temperature. In the present study, we study the temperature dependence of ac conductivity and dielectric properties of Au/Si_3N_4/n-Si (MIS) structure in a temperature range of 80 K–400 K at two different frequencies.

2. Experimental details

Au/Si_3N_4/n-Si (MIS) structures were fabricated on phosphorus doped (n-type) single crystal Si substrates each with a 2-inch diameter (1 inch = 2.54 cm), 300-μm thickness, (100) orientation, and 0.5-Ω·cm resistivity. For the fabrication process, the n-Si substrates were chemically cleaned using the conventional method and then chemically etched and finally quenched in deionized water. Prior to each cleaning step, the Si substrate was rinsed thoroughly in deionized water of resistivity of 18 MΩ·cm using an ultrasonic bath. After cleaning and etching steps, the Si substrates were mounted on a stainless steel sputtering holder that was heated optically and loaded into a radio frequency (RF) magnetron sputtering system. The Si substrate was heated up to 400 °C in 1×10^{8}-mbar (1 bar = 10^5 Pa) high vacuum and sputter cleaned in pure argon ambient to ensure the removal of any residual organic substance. Then, the silicon nitride (Si_3N_4) film was deposited on n-Si using a high purity (99.999%) silicon nitride target. In addition, the film was deposited at a constant pressure of 3×10^{-3} mbar and a constant substrate temperature of 200 °C.

The ohmic and rectifier contacts were formed using a

*Projected supported by Gazi University Scientific Research Project (BAP), FEF. 05/2012-15.

†Corresponding author. E-mail: ademt@gazi.edu.tr

© 2013 Chinese Physical Society and IOP Publishing Ltd

thermal evaporation system. The ohmic back contacts were formed by the deposition of high-purity Au (99.999%) with a thickness of ~2000 Å at 450 °C, under 10^{-7}-mbar vacuum and the sample was annealed at 400 °C to achieve a good ohmic contact behavior. After that, circular dot shaped rectifier front contacts with 1-mm diameter and ~2000 Å-thickness were formed by the deposition of high-purity Au onto Si_3N_4 thin film at 50 °C. In this way, Au/Si_3N_4/n-Si (MIS) structures were fabricated for the electrical measurements. The electrode connections were made by silver paste. The interfacial insulator layer thickness was estimated to be about 85 Å from measurement of the insulator capacitance in the strong accumulation region for the MIS structure.

The capacitance–voltage (C–V) and conductance–voltage (G/ω–V) characteristics were investigated in the temperature range of 80 K–400 K at 100 kHz and 1 MHz, by using an HP 4192A LF impedance analyser (5 Hz–13 MHz) and a small ac test signal 50 mV_{rms} from an external pulse generator applied to the sample in order to meet the requirement. All measurements were controlled by using a Janes vpf-475 cryostat, which enables us to make measurements in a temperature range of 77 K–450 K. The sample temperature was always monitored by using a copper-constantan thermocouple close to the sample and by measuring with a dmm/scanner Keithley model 199 and a Lake Shore model 321 auto-tuning temperature controller with sensitivity better than ±0.1 K. In addition, the entire measurements were performed using a microcomputer through an IEEE-488 AC/DC converter card.

3. Results and discussion

3.1. Temperature-dependent C–V and G/ω–V measurements at 100 kHz and 1 MHz

Admittance spectroscopy is a technique of measuring the admittance, i.e., capacitance (C) and conductance (G). The C and G/ω measurements of the Au/Si_3N_4/n-Si (MIS) structure were carried out in the temperature range of 80 K–400 K at 100 kHz and 1 MHz. The variations of capacitance with temperature are presented in Figs. 1(a) and 1(b), respectively. As shown in Figs. 1(a) and 1(b), the values of capacitance increase with temperature increasing. The increase in capacitance with temperature may be due to the interfacial space-charge formation.[21–24] In addition, the value of capacitance increases with the frequency decreasing. The high values of the capacitance at low frequencies result from the presences of the interface states at metal/semiconductor interface. In other words, at low frequencies, the interface states can follow the alternating current (ac) signal and yield an excess capacitance and conductance. However, at high frequencies, the charges at the interface states cannot follow the ac signal and cannot contribute to the total capacitance.[24,25] The variations of conductance with temperature at 100 kHz and 1 MHz are shown in Figs. 2(a) and 2(b), respectively. As shown in Figs. 2(a) and 2(b), the values of conductance increase with the temperature increasing, but decrease with frequency increasing. The increase in conductance with temperature may be due to the thermally activated charge carrier mobility.

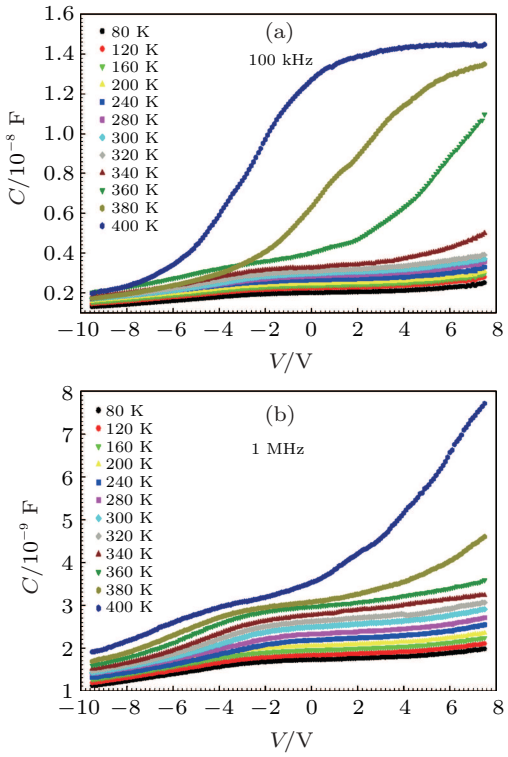


Fig. 1. (color online) Variations of the capacitance (C) with temperature at (a) 100 kHz and (b) 1 MHz for MIS structure.

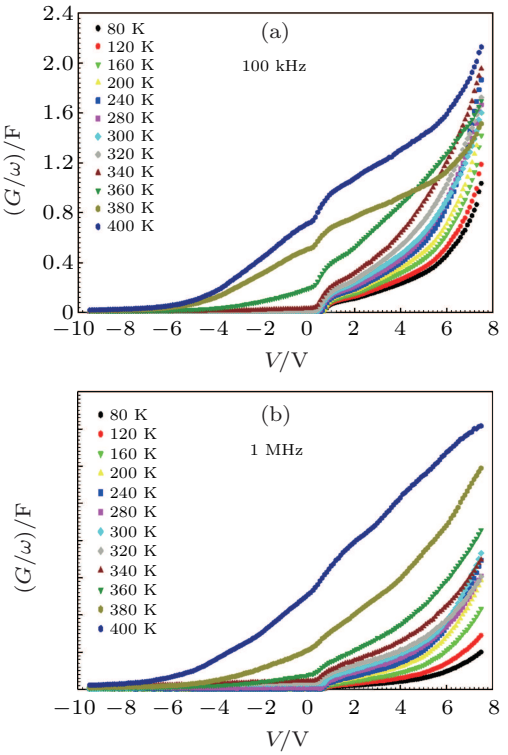


Fig. 2. (color online) Variations of the conductance (G/ω) with temperature at (a) 100 kHz and (b) 1 MHz for the MIS structure.

3.2. Temperature-dependent dielectric properties at 100 kHz and 1 MHz

The complex permittivity can be defined in the following complex form:[26,27]

$$\varepsilon^*(\omega) = \varepsilon'(\omega) - \mathrm{i}\varepsilon''(\omega), \tag{1}$$

where ε' and ε'' are the real and the imaginary parts of the complex permittivity, and i is the square root of -1. The real part of the permittivity, $\varepsilon'(\omega)$, is a measure of the energy stored from the applied electric field in the material and identifies the strength of alignment of dipoles in the dielectric. The imaginary part of the permittivity, $\varepsilon''(\omega)$, or a loss factor, is the energy dissipated in the dielectric, which is associated with the frictional dampening that prevents the displacement of bound charge from keeping in phase with the field change.[28]

The complex permittivity formalism is employed to describe the electrical and dielectric properties. In the ε^* formalism, in the case of admittance measurements, the following relation holds:

$$\varepsilon^* = \frac{Y^*}{\mathrm{i}\omega C_0} = \frac{C}{C_0} - \mathrm{i}\frac{G}{\omega C_0}, \tag{2}$$

where Y^*, C, and G are the measured admittance, capacitance, and conductance values of the dielectric material, respectively, and ω is the angular frequency ($\omega = 2\pi f$) of the applied electric field, C_0 is the capacitance of an empty capacitor and expressed as $C_0 = \varepsilon_0 A/d$, with $A(= 7.85 \times 10^{-3}\ \mathrm{cm}^2)$ being the rectifier contact area in cm^2, d is the interfacial insulator layer thickness, and ε_0 is the permittivity of free space charge ($\varepsilon_0 = 8.85 \times 10^{-14}$ F/cm).

The real part of the complex permittivity, the dielectric constant (ε'), is calculated using the capacitance values which are measured at the forward bias voltage of about 1 V from the relation[29,30]

$$\varepsilon'(\omega) = \frac{C_\mathrm{m}}{C_0}, \tag{3}$$

where C_m is the measured maximal capacitance of the MIS structure in the strong accumulation region. The insulator layer thickness d (= 85 Å) calculated from C–V characteristics using the equation $C_\mathrm{ox} = \varepsilon_\mathrm{i}\varepsilon_0 A/d$, where C_ox is the capacitance of the interfacial layer, and $\varepsilon_\mathrm{i} = 7.5\varepsilon_0$ and $\varepsilon_\mathrm{s} = 11.9\varepsilon_0$[2] are the permittivities of the interfacial insulator layer (Si_3N_4) and semiconductor (Si), respectively.

On the other hand, the imaginary part of the complex permittivity, the dielectric loss (ε''), is calculated using the measured conductance values from the relation

$$\varepsilon''(\omega) = \frac{G_\mathrm{m}}{\omega C_0}, \tag{4}$$

where G_m is the measured maximal conductance of MIS structure in the strong accumulation region. The dissipation factor or loss factor tangent ($\tan\delta$), which means the phase difference due to the loss of energy within the structure, can be expressed as follows:[26–31]

$$\tan\delta = \frac{\varepsilon''(\omega)}{\varepsilon'(\omega)}. \tag{5}$$

The ac conductivity is calculated from the dielectric loss values according to the relation

$$\sigma^* = \mathrm{i}\varepsilon_0\omega\varepsilon^*(\omega) = \mathrm{i}\varepsilon_0\omega(\varepsilon' - \mathrm{i}\varepsilon'') = \varepsilon_0\omega\varepsilon'' + \mathrm{i}\varepsilon_0\omega\varepsilon'. \tag{6}$$

The real part of the complex conductivity (σ^*) is calculated using the relation

$$\sigma_\mathrm{ac} = \omega C \tan\delta(d/A) = \varepsilon_0\omega\varepsilon''. \tag{7}$$

As it turns out, the effect of conductivity can be highly suppressed when the data are presented in the modulus representation. The electric modulus approach began when the reciprocal complex permittivity was discussed as an electrical analogue to the mechanical shear modulus.[32] From the physical point of view, the electrical modulus corresponds to the relaxation of the electric field in the material when the electric displacement remains constant. Therefore, the modulus represents the real dielectric relaxation process.[33,34] The complex modulus $M^*(\omega)$ was introduced to describe the dielectric response of non-conducting material. This formalism has been applied also to materials with non-zero conductivities. The starting point for further consideration is the definition of the dielectric modulus[32,35]

$$M^*(\omega) = \frac{1}{\varepsilon^*} = M'(\omega) + \mathrm{i}M''(\omega). \tag{8}$$

$$M'(\omega) = \frac{\varepsilon'(\omega)}{\varepsilon'(\omega)^2 + \varepsilon''(\omega)^2},$$

and

$$M''(\omega) = \frac{\varepsilon''(\omega)}{\varepsilon'(\omega)^2 + \varepsilon''(\omega)^2}, \tag{9}$$

where M' and M'' are the real and the imaginary parts of complex modulus. Based on Eq. (9), we change the forms of presentation of the dielectric data from ε' (ω) and ε'' (ω) to M' (ω) and M'' (ω).

The temperature dependences of the ε', ε'', $\tan\delta$, σ_ac, M', and M'' of the Au/Si_3N_4/n-Si (MIS) structure are obtained from C–V and G/ω–V data at 100 kHz and 1 MHz in the temperature range of 80 K–400 K. The variations of dielectric parameters with temperature are shown in Figs. 3(a)–3(c), respectively. As can be seen from these figures, the values of ε', ε'', and $\tan\delta$ increase exponentially as the temperature increases at a high temperature range of 300 K–400 K. On the other hand, these values keep almost constant at a low temperature range of 80 K–280 K. As temperature rises, imperfections/disorders are created in the lattice and the mobility of the majority charge carriers (ions and electrons) increases.[7,21,31,36–40]

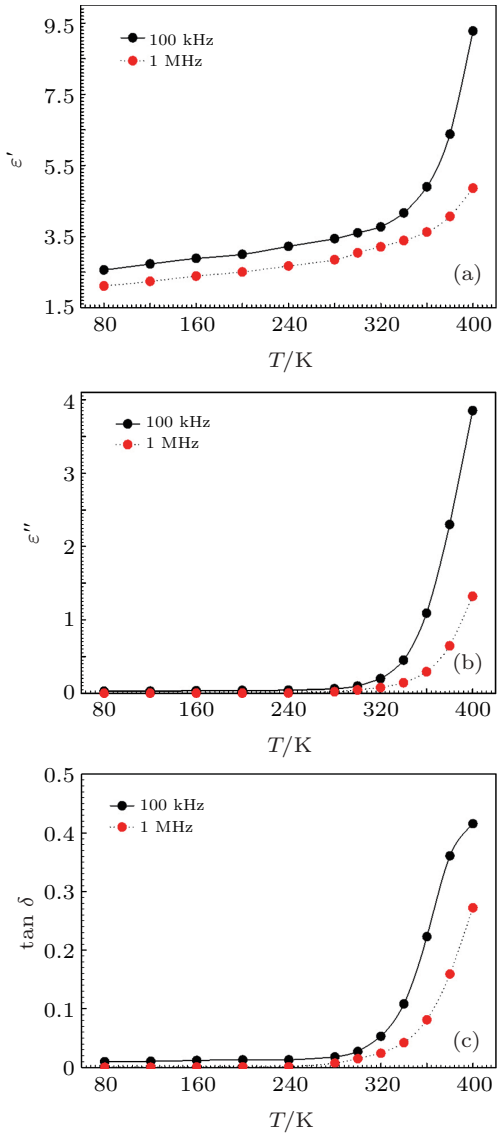


Fig. 3. (color online) Variations of the ε' (a), ε'' (b), and tanδ (c) with temperature at 100 kHz and 1 MHz for the MIS structure.

In addition, the ε' and ε'' decrease with frequency increasing at all temperatures exhibiting a similar trend with the capacitance and conductance. These curves closely resemble those predicted by the Debye relaxation model for orientational polarization.[41] Furthermore, the decreases in ε' and ε'' with the increasing frequency are explained by the fact that as the frequency is raised, the interfacial dipoles have less time to orient themselves in the direction of the alternating field.[38–40]

Figure 4 shows the temperature dependences of ac conductivity (σ_{ac}) measured at two frequencies (100 kHz and 1 MHz). It is evident that σ_{ac} is both frequency and temperature dependent and increases with frequency and temperature increasing. As shown in Fig. 4, the values of ac conductivity keep almost constant at a low temperature range (80 K–280 K) for the two frequencies and increase exponentially at a high temperature range (300 K–400 K). The increase in σ_{ac} with temperature increasing is attributed to the impurities or dislocations at metal/semiconductor interface.[38–43] Furthermore, the frequency dependence of conductivity in the relaxation phenomenon are caused by the the mobile charge carriers.

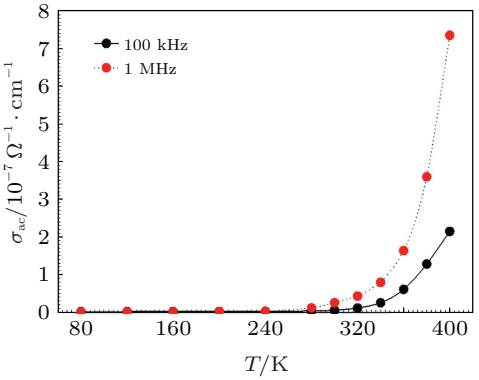


Fig. 4. (color online) Temperature dependences of ac conductivity (σ_{ac}) for two different frequencies.

In the case of a thermally activated electrical conduction, the temperature dependence of ac conductivity can be explained according to the Arrhenius equation

$$\sigma_{ac} = \sigma_0 \exp\left(\frac{-E_a}{kT}\right), \tag{10}$$

where σ_0 is called the pre-exponential factor and E_a is called the activation energy for ac electrical conduction mechanism.[31,33,38,40,43–49] The E_a is determined from the slope of the straight lines in the resulting plots at two different frequencies (see Fig. 5). Figure 5 shows the Arrhenius plots (lnσ_{ac} versus 1000/T) for the temperature dependence of ac conductivity $\sigma_{ac}(T)$ measured at 100 kHz and 1 MHz under accumulation bias in the temperature range of 80 K–400 K. As can be seen from Fig. 5, lnσ_{ac} versus 1000/T plots for two frequencies show two linear regions with two different slopes which correspond to region 1 (80 K–240 K) and region 2 (280 K–400 K). The values of E_a for the conduction process are calculated to be 5 meV and 347 meV at the low temperature (between 80 K and 240 K) and high temperature (between 280 K and 400 K) for 100 kHz, respectively. The values of E_a are calculated to be 10 meV and 365 meV for 1 MHz. As a result, the value of activation energy increases with the temperature and frequency increasing.

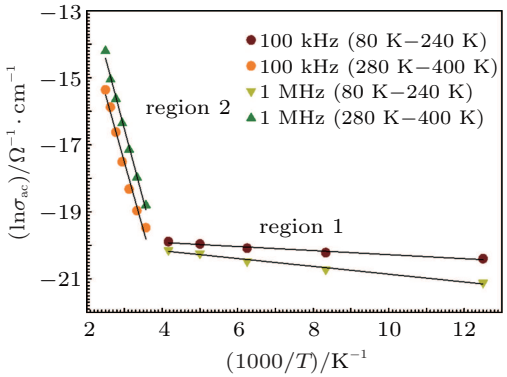


Fig. 5. (color online) Arrhenius plots of ac conductivity for MIS structure at several different frequencies.

The real (M') and imaginary (M'') parts of electric modulus (M^*) are calculated from ε' and ε''. The temperature dependences of the M$'$ and M'' of MIS structure are shown in Figs. 6(a) and 6(b), respectively. As seen in Fig. 6(a), the value of M' decreases with the temperature increasing, but increases with frequency increasing. This dependence indicates that the dielectric constant of the structure is thermally activated. The imaginary part of electric modulus is indicative of energy loss in the structure under electrical field. As seen in Fig. 6(b), the values of M'' increase with temperature increasing at above 280 K while keeping almost constant in the low temperature range.[21,31,33,50–53]

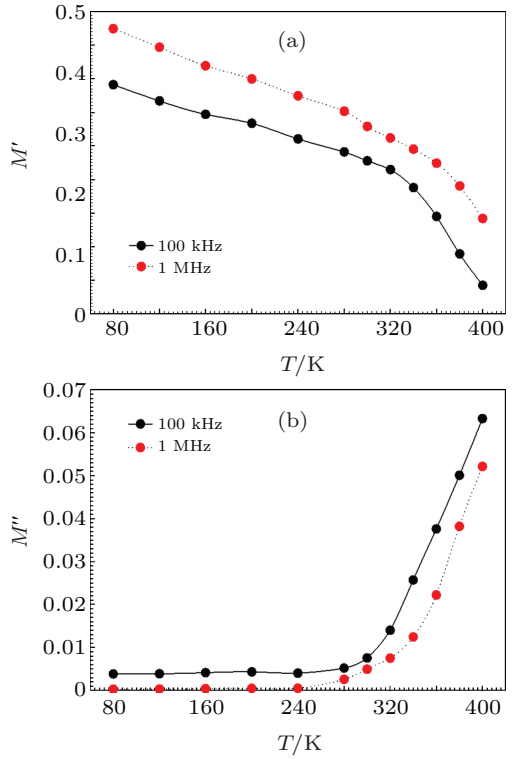


Fig. 6. (color online) Variations of real part (M') (a) and imaginary part (M'') (b) of electric modulus (M^*) with temperature at two different frequencies.

4. Conclusions

In the present work, the temperature dependences of dielectric properties and ac conductivity of the Au/Si_3N_4/n-Si (MIS) structure are investigated by using admittance measurements. The values of ε' and ε'' increase with temperature increasing, but decrease with frequency increasing. As the applied field is lowered, significant decreases in the values of ε' and ε'' occur. Frequency and temperature dependences of ε' are attributed to interfacial and orientational polarizations, whereas that of ε'' is associated with the conduction loss. The value of σ_{ac} increases with frequency and temperature increasing. The increase in the σ_{ac} with temperature increasing is attributed to the impurities or dislocations at the metal–semiconductor interface. In addition, the activation energies for two frequencies are obtained from the Arrhenius plots. The value of activation energy of the MIS structure for conduction process is found to increase with temperature and frequency increasing. The observed temperature dependent capacitance and conductance behaviours suggest that the conduction mechanism in MIS structure may be due to the hopping of charge carriers between the distributed defects/localized states under the effect of temperature.

References

[1] Kano K 1998 *Semiconductor Devices* (New Jersey: Prentice-Hall Inc.)
[2] Sze S M 1981 *Physics of Semiconductor Devices* 2nd edn. (New York: John Wiley& Sons)
[3] Nicollian E H and Brews J R 1982 *MOS (Metal Oxide Semiconductor) Physics and Technology* (New York: John Wiley & Sons)
[4] Sztkowski J and Sieranski K 1992 *Solid State Electron.* **35** 1013
[5] Cova P, Singh A and Masut R A 1997 *J. Appl. Phys.* **82** 5217
[6] Chattopadhyay P and Raychaudhuri B 1993 *Solid State Electron.* **36** 605
[7] Tataroğlu A 2006 *Microelectron. Eng.* **83** 2551
[8] Hudait M K and Krupanidhi S B 2000 *Solid State Electron.* **44** 1089
[9] Inoue N, Lichtenwalner D J, Jur J S and Kingon A I 2007 *Jap. J. Appl. Phys.* **46** 6480
[10] Karataş Ş and Türüt A 2010 *Microelectron. Reliab.* **50** 351
[11] Tataroğlu A and Altındal Ş 2008 *Microelectron. Eng.* **85** 1866
[12] Ataseven T, Tataroğlu A, Memmedli T and Özçelik S 2012 *J. Optoelectron. Adv. Mater.* **14** 640
[13] Bülbül M M 2007 *Microelectron. Eng.* **84** 124
[14] Wang L, Wang X S, Tang J C and Cue N 2002 *Mater. Charact.* **48** 189
[15] Jung S B, Park S W, Yang J K, Park H H and Kim H 2004 *Thin Solid Films* **447–448** 580
[16] Miyazaki H, Yoshizawa Y I and Hirao K 2008 *Mater. Sci. Eng. B* **148** 257
[17] Karazhanov S Z, Kroll P, Marstein E S and Holt A 2010 *Thin Solid Films* **518** 4918
[18] Pham T A, Li T, Shankar S, Gygi F and Gali G 2010 *Appl. Phys. Lett.* **96** 062902
[19] Awan S A and Gould R D 2003 *Thin Solid Films* **423** 267
[20] Elmiger J R, Schieck R and Kunst M 1997 *J. Vac. Sci. Technol. A* **15** 2418
[21] Dökme İ and Altındal S 2011 *IEEE Trans. Electron Dev.* **58** 4042
[22] Eroğlu A, Tataroğlu A and Altındal Ş 2012 *Microelectron. Eng.* **91** 154
[23] Kaya A, Altındal Ş, Şafak A Y and Sönmez Z 2013 *Chin. Phys. Lett.* **30** 017301
[24] Yahia I S, Farag A A M, Yakuphanoğlu F and Farooq W A 2011 *Synthetic Metals* **161** 881
[25] Ertuğrul R and Tataroğlu A 2012 *Chin. Phys. Lett.* **29** 077304
[26] Symth C P 1955 *Dielectric Behaviour and Structure* (New York: McGraw-Hill)
[27] Daniel V V 1967 *Dielectric Relaxation* (London: Academic Press)
[28] Cheng D 1989 *Field and Wave Electromagnetics* 2nd Edn. (New York: Addison-Wesley)
[29] Popescu M and Bunget I 1984 *Physics of Solid Dielectrics* (Amsterdam: Elsevier)
[30] Chelkowski A 1980 *Dielectric Physics* (Amsterdam: Elsevier)
[31] Tataroğlu A and Altındal Ş 2007 *Nucl. Instr. Meth. B* **254** 113
[32] McCrum N G, Read B E and Williams G 1967 *Anelastic and Dielectric Effects in Polymeric Solids* (New York: Wiley)
[33] Dökme İ, Altındal Ş, Tunç T and Uslu İ 2010 *Microelectron. Reliab.* **50** 39
[34] Yücedağ İ, Altındal Ş and Tataroğlu A 2007 *Microelectron. Eng.* **84** 180
[35] Yakuphanoğlu F, Yahia I S, Senkald B F, Sakrc G B and Farooq W A 2011 *Synthetic Metals* **161** 817
[36] Prabakar K, Narayandass S K and Mangalaraj D 2003 *Phys. Stat. Sol. (a)* **199** 507
[37] Abdel K M M, Elzayat M Y, Hammad T R, Aboud A I and Abdelmonem H 2011 *Phys. Scr.* **83** 035705
[38] Sattar A A and Rahman S A 2003 *Phys. Stat. Sol. (a)* **200** 415
[39] Maurya D, Kumar J and Shripal 2005 *J. Phys. Chem. Solids* **66** 1614

[40] Maity S, Bhattacharya D and Ray S K 2011 *J. Phys. D: Appl. Phys.* **44** 095403
[41] Matheswaran P, Sathyamoorthy R, Saravanakumar R and Velumani S 2010 *Mater. Sci. Eng., B* **174** 269
[42] Migahed M D, Ishra M, Fahmy T and Barakat A 2004 *J. Phys. Chem. Solids* **65** 1121
[43] Farag A A M, Mansour A M, Ammar A H, Abdel R M and Farid A M 2012 *J. Alloys Compd.* **513** 404
[44] Sharma R S, Mehta N and Kumar A 2008 *Chin. Phys. Lett.* **25** 4079
[45] Kungumadevi L, Sathyamoorthy R and Subbarayan A 2010 *Solid State Electron.* **54** 58
[46] Kim J S, Lee H J, Lee S Y, Kim I W and Lee S D 2010 *Thin Solid Films* **518** 6390
[47] Senthilarasu S, Sathyamoorthy R, Ascencio J A, Lee S H and Hahn Y B 2007 *J. Appl. Phys.* **101** 034111
[48] Yahia I S, Abd El-sadek M S and Yakuphanoğlu F 2012 *Dyes Pigment.* **93** 1434
[49] Meena P, Balasubramanian C, Narayandass S K and Mangalaraj D 1993 *Phys. Stat. Sol. (a)* **135** 207
[50] Mohamed M B, Wang H and Fuess H 2010 *J. Phys. D: Appl. Phys.* **43** 455409
[51] Tataroğlu A, Yücedağ İ and Altındal S 2008 *Microelectron. Eng.* **85** 1518
[52] Vinoth R S and Govindaraj G 2010 *Solid State Ionics* **181** 504
[53] Singh N, Agarwal A and Sanghi S 2011 *Current Appl. Phys.* **11** 783